

Supporting Information (SI)

One step synthesis of nitrogen-rich green primary explosives from secondary: synthesis, characterization, and performance study

Parasar Kumar,^a Vikas D. Ghule,^b Srinivas Dharavath ^{a*}

^aEnergetic Materials Laboratory, Department of Chemistry, Indian Institute of Technology Kanpur, Kanpur-208016, Uttar Pradesh, India.

E-mail: srinivasd@iitk.ac.in

^bDepartment of Chemistry, National Institute of Technology Kurukshetra, Kurukshetra-136119, Haryana, India.

Table of Contents

General methods	S2
Experimental conditions	S2-S5
Crystal Structure for 2.	S5-S8
NMR, IR, HRMS spectrum & TGA-DSC plots for 2 to 6.	S8-S18
Computational Details	S19-S25
References	S26

Caution! All the compounds investigated are potentially explosive, energetic materials. Although we have experienced no difficulties in syntheses and characterization of these compounds, manipulations must be carried out by using appropriate standard safety precautions. Eye protection and leather gloves must be always worn.

General Methods.

Reagents were purchased from Ak Scientifics, Acros Organics or Aldrich as analytical grade and were used as received. ^1H NMR, ^{13}C NMR spectra were recorded using JEOL DELTA (ECS) 500 (^1H , 500 MHz; ^{13}C , 126 MHz) nuclear magnetic resonance spectrometer. DMSO- d_6 was employed as the solvent and locking solvent. All the synthesized compound showed different colour which may be attributed to the variable extent of conjugation in molecule which are in different electronic environment and possess different energy gap. Chemical shifts are given relative to $(\text{CH}_3)_4\text{Si}$ for ^1H and ^{13}C spectra. Decomposition temperatures (onset) were recorded using a dry nitrogen gas purge and at heating rate of $5\text{ }^\circ\text{C min}^{-1}$ on a differential scanning calorimeter (SDT650). IR spectra were recorded using Zn-Se pellets with ECO-ATR spectrometer (Bruker Alpha II). Density was determined at room temperature by employing Anton Par Ultra5000 gas pycnometer in helium atmosphere. Impact and friction-sensitivity measurements were tested by employing a standard BAM Fall hammer and a BAM friction tester. The single-crystal X-ray data collection was carried out using Bruker APEX-II CCD diffractometer. The crystal was kept at 100 K during data collection.

Experimental Section:

Synthesis of 4,4',5,5'-tetranitro-1H,1'H-2,2'-biimidazole (1): Compound **1** was prepared according to the literature procedure.^{1,2}

General synthesis of 5-azido-4,4',5'-trinitro-1H,1'H-2,2'-biimidazole (2) and 5,5'-diazido-4,4'-dinitro-1H,1'H-2,2'-biimidazole (6): To the solution of compound **1** (400 mg, 1.27 mmol) in 10 mL of distilled water at room temperature, ZnCl_2 (207 mg, 1.51 mmol; 340 mg, 2.4 mmol) was added with uniform stirring followed by the addition of NaN_3 (99 mg, 1.5 mmol; 413 mg, 6.35 mmol). The reaction mixture was then heated to $80\text{ }^\circ\text{C}$ for 5 hours. The reaction mixture was then removed and allowed to cool to room temperature followed by acidification using conc. HCl (15 %) to $\text{pH}=1$. After two hours of acidification, precipitate was observed which was filtered and washed with cold water, dried in oven at $50\text{ }^\circ\text{C}$.

Synthesis of 5-azido-4,4',5'-trinitro-1H,1'H-2,2'-biimidazole (2): Yellow. Yield 70 % (276 mg, 0.86 mmol). $T_d(\text{onset})$: 252 °C. $^1\text{H NMR}$ (500 MHz, DMSO- d_6): δ (ppm) 6.22 (br, 2H). $^{13}\text{C NMR}$ (126 MHz, DMSO- d_6): δ (ppm) 131.0, 135.2, 138.3, 138.8, 140.6, 142.8. IR (ATR, ZnSe, cm^{-1}): 522, 754, 1189, 1330, 1405, 1552, 1619, 2140, 2894. MS (ESI) m/z : calculated for $\text{C}_6\text{H}_2\text{N}_{10}\text{O}_6$ [M $^+$] 310.01; found 310.13; [M+H] 311.02; found 311.13. Elemental analysis: (%) calculated for $\text{C}_6\text{H}_2\text{N}_{10}\text{O}_6 \cdot 1.4\text{H}_2\text{O}$ (310.14): C, 21.49; H, 1.44; N, 41.77; found C, 22.91; H, 1.48; N, 41.29.



Synthesis of 5,5'-diazido-4,4'-dinitro-1H,1'H-2,2'-biimidazole (6): Brown. Yield 60 % (234 mg, 0.76 mmol). $T_d(\text{onset})$: 121 °C. $^1\text{H NMR}$ (500 MHz, DMSO- d_6): δ (ppm) 4.31 (br, 2H). $^{13}\text{C NMR}$ (126 MHz, DMSO- d_6): We have tried getting $^{13}\text{C NMR}$ for this compound, but it is getting sudden precipitated within hour. Hence, we are not able to observe the carbon peaks. IR (ATR, ZnSe, cm^{-1}): 914, 1103, 1180, 1333, 1408, 1551, 2145, 3534. MS (ESI) m/z : calculated for $\text{C}_6\text{H}_2\text{N}_{12}\text{O}_4$ [M-H] 305.02; found 305.15. Elemental analysis: (%) calculated for $\text{C}_6\text{H}_2\text{N}_{12}\text{O}_4$ (306.16): C, 23.54; H, 0.66; N, 54.90; found C, 23.60; H, 0.64; N, 54.26.



Table S1: Optimisation conditions for the synthesis of compounds **2** and **6**.

S. No	Solvent	Additives	Yield (%)
1.	Acetone	-	No reaction
2.	water	-	No reaction
3.	DMSO	-	No reaction
4.	Acetone + water	-	No reaction
5.	Acetone	ZnCl_2	No reaction

6.	water	ZnCl ₂	70
----	-------	-------------------	----

General procedure for the synthesis of salts 3-5: Compound **2** (50 mg, 0.16 mmol) was taken in methanol (5 ml) and hydroxyl amine hydrate (18 mg, 0.35 mmol), hydrazine monohydrate (18 mg, 0.36 mmol), and 3,5-diamino-4*H*-1,2,4-triazole (DAT) (36 mg, 0.36 mmol) was added into it and stirred at room temperature for 12 hours. The formed precipitate was collected by filtration and washed with methanol and dried in air to get pure products in quantitative yields.

Synthesis of dihydroxylammonium-5-azido-4,4',5'-trinitro-[2,2'-biimidazole]-1,1'-diide (3) : Brick red. Yield 80 % (48 mg, 0.12 mmol). T_d(onset): 245 °C. ¹H NMR (500 MHz, DMSO-d₆): δ (ppm) 7.55 (br). ¹³C NMR (126 MHz, DMSO-d₆): δ(ppm) 134.8, 138.9, 139.1, 140.3, 144.5, 146.1. ¹⁵N NMR (51 MHz, DMSO-d₆): δ(ppm) -25.91, -35.40, -105.21, -117.28, -123.02, -129.06, -157.03, -187.09, -231.50, -276.70. IR (ATR, ZnSe, cm⁻¹): 701, 753, 809, 1000, 1185, 1300, 1324, 1410, 1495, 1651, 2129, 3244. Elemental analysis: (%) calculated for C₆H₈N₁₂O₈ (376.20): C, 19.16; H, 2.14; N, 44.68; found C, 19.48; H, 2.23; N, 44.39.



Synthesis of dihydrazinium-5-azido-4,4',5'-trinitro-[2,2'-biimidazole]-1,1'-diide (4) : Brick red. Yield 87 % (52 mg, 0.14 mmol). T_d(onset): 131 °C. ¹H NMR (500 MHz, DMSO-d₆): δ (ppm) 7.27 (br). ¹³C NMR (126 MHz, DMSO-d₆): δ(ppm) 135.0, 139.3, 140.2, 144.1, 145.7, 146.4. IR (ATR, ZnSe, cm⁻¹): 578, 692, 954, 1092, 1192, 1291, 1349, 1492, 1620, 2122, 3328. Elemental analysis: (%) calculated for C₆H₁₀N₁₄O₆·1.6H₂O (374.23): C, 17.88; H, 3.30; N, 48.65; found C, 18.03; H, 3.37.; N, 48.77.



Synthesis of di-3,5-diamino-4H-1,2,4-triazol-1-ium-5-azido-4,4',5'-trinitro-[2,2'-biimidazole]-1,1'-diide (5): Dark brown. Yield 83% (68 g, 0.13 mmol). T_d (onset): 120 °C. ^1H NMR (500 MHz, DMSO- d_6): δ (ppm) 6.26 (br). ^{13}C NMR (126 MHz, DMSO- d_6): δ (ppm) 132.1, 133.6, 137.9, 140.2, 140.6, 141.1, 153.4. IR (ATR, ZnSe, cm^{-1}): 522, 793, 847, 1000, 1187, 1293, 1399, 1490, 1649, 2128, 3359. Elemental analysis: (%) calculated for $\text{C}_{10}\text{H}_{12}\text{N}_{20}\text{O}_6 \cdot 2\text{H}_2\text{O}$ (508.12): C, 22.06; H, 2.96; N, 51.56; found C, 22.30; H, 2.41; N, 49.00.

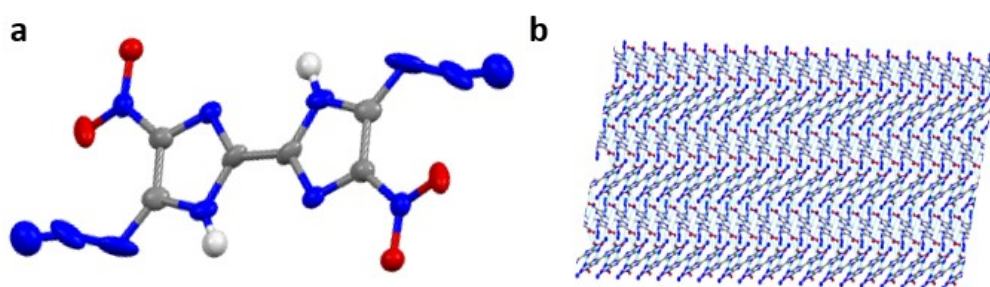


Figure S1: Crystal structure, and crystal packing (with weak interactions) of **6**.

Table S2: Crystallographic data for 6.

CCDC No.	2312111
Empirical formula	$\text{C}_6\text{H}_{13}\text{N}_{12}\text{O}_{11}$
Formula weight	429.244
Temperature/K	100
Crystal system	monoclinic
Space group	Pc
$a/\text{\AA}$	10.6901(9)
$b/\text{\AA}$	6.3378(6)
$c/\text{\AA}$	12.8174(13)
$\alpha/^\circ$	90
$\beta/^\circ$	104.095(3)
$\gamma/^\circ$	90
Volume/ \AA^3	842.26(14)
Z	2
$\rho_{\text{calc}}/\text{g cm}^{-3}$	1.693
μ/mm^{-1}	0.159
$F(000)$	442.3
Crystal size/ mm^3	$0.1 \times 0.1 \times 0.1$

Radiation	Mo K α ($\lambda = 0.71073$)
2 Θ range for data collection/ $^{\circ}$	6.42 to 56.58
Index ranges	$-14 \leq h \leq 14, -8 \leq k \leq 8, -14 \leq l \leq 17$
Reflections collected	13670
Independent reflections	3787 [Rint = 0.0344, Rsigma = 0.0343]
Data/restraints/parameters	3787/2/284
Goodness-of-fit on F2	1.049
Final R indexes [$I \geq 2\sigma(I)$]	R1 = 0.0596, wR2 = 0.1628
Final R indexes [all data]	R1 = 0.0737, wR2 = 0.1780
Largest diff. peak/hole / e \AA^{-3}	0.65/-0.75
Flack parameter	-0.4(19)

Table S3: Fractional Atomic Coordinates ($\times 10^4$) and Equivalent Isotropic Displacement Parameters ($\text{\AA}^2 \times 10^3$) for **6**. U_{eq} is defined as 1/3 of the trace of the orthogonalised U_{ij} tensor.

Atom	x	y	z	U(eq)
O1	6139(2)	6216(4)	1758.6(19)	33.6(5)
O2	4163(3)	6845(6)	1752(2)	48.5(7)
N1	5459(2)	2536(4)	681.2(19)	27.4(5)
N3	4995(3)	5698(5)	1566.2(19)	31.2(5)
N2	3533(2)	966(5)	383(2)	33.2(5)
N4	2250(3)	3182(6)	1129(4)	55.7(11)
N5	2250(3)	4290(8)	1939(4)	59.1(11)
N6	1965(5)	5070(7)	2527(5)	67.3(11)
C2	4619(3)	3698(5)	1082(2)	30.7(6)
C1	4775(3)	871(5)	275(2)	32.0(6)
C3	3429(3)	2785(5)	917(3)	32.1(6)

Table S4: Anisotropic Displacement Parameters ($\text{\AA}^2 \times 10^3$) for **6**. The Anisotropic displacement factor exponent takes the form: $-2\pi^2[h2a*2U_{11}+2hka*b*U_{12}+...]$.

Atom	U11	U22	U33	U23	U13	U12
O1	32.1(10)	32.4(10)	35.8(11)	-0.1(8)	7.5(8)	-3.8(8)
O2	42.2(13)	77.0(19)	25.6(10)	-2.8(11)	6.9(9)	20.2(13)
N1	30.1(11)	29.7(12)	19.9(10)	5.0(8)	1.5(8)	-5.2(9)
N3	34.8(12)	37.8(13)	21.6(9)	1.1(10)	7.8(9)	-2.4(10)
N2	26.9(11)	34.5(13)	32.1(11)	7.6(10)	-4.3(9)	-6.7(9)
N4	22.2(12)	49.5(18)	93(3)	36(2)	9.8(15)	-8.2(12)
N5	30.0(15)	83(3)	70(3)	31(2)	23.1(16)	18.2(16)
N6	66(3)	77(3)	65(2)	4(2)	27(2)	-5(2)
C2	30.2(13)	34.4(13)	26.4(12)	7.7(11)	4.9(10)	-5.9(11)
C1	41.2(15)	24.9(13)	26.6(12)	2.1(11)	1.8(11)	-14.3(11)
C3	32.5(14)	27.7(13)	32.9(13)	14.7(11)	1.4(11)	-1.8(11)

Table S5: Bond Lengths for **6**.

Atom	Atom	Length/ \AA	Atom	Atom	Length/ \AA
O1	N3	1.232(4)	N2	C3	1.359(5)

O2	N3	1.216(4)	N4	N5	1.253(7)
N1	C2	1.356(4)	N4	C3	1.376(5)
N1	C1	1.317(4)	N5	N6	1.008(7)
N3	C2	1.426(4)	C2	C3	1.365(4)
N2	C1	1.369(4)	C1	C11	1.453(7)

Table S6: Bond Angles for **6**.

Atom	Atom	Atom	Angle/°	Atom	Atom	Atom	Angle/°
C1	N1	C2	103.3(3)	N1	C2	C3	112.9(3)
O1	N3	C2	119.0(3)	C3	C2	N3	126.6(3)
O2	N3	O1	122.6(3)	N1	C1	N2	112.5(3)
O2	N3	C2	118.3(3)	N1	C1	C11	125.7(4)
C3	N2	C1	106.8(3)	N2	C1	C11	121.7(3)
N5	N4	C3	116.8(3)	N2	C3	N4	116.5(3)
N6	N5	N4	162.6(5)	N2	C3	C2	104.5(3)
N1	C2	N3	120.3(3)	C2	C3	N4	139.1(4)

Table S7: Torsion Angles for **6**.

A	B	C	D	Angle/°	A	B	C	D	Angle/°
O1	N3	C2	N1	-10.6(4)	C2	N1	C1	N2	1.4(3)
O1	N3	C2	C3	172.7(3)	C2	N1	C1	C11	179.0(4)
O2	N3	C2	N1	167.9(3)	C1	N1	C2	N3	-177.8(3)
O2	N3	C2	C3	-8.8(4)	C1	N1	C2	C3	-0.7(3)
N1	C2	C3	N2	-0.2(3)	C1	N2	C3	N4	-179.0(3)
N1	C2	C3	N4	179.8(4)	C1	N2	C3	C2	1.0(3)
N3	C2	C3	N2	176.7(3)	C3	N2	C1	N1	-1.6(3)
N3	C2	C3	N4	-3.3(6)	C3	N2	C1	C11	-179.3(3)
N5	N4	C3	N2	152.4(3)	C3	N4	N5	N6	-174.9(16)
N5		N4		C3		C2			-27.7(6)

Table S8: Hydrogen Atom Coordinates ($\text{\AA} \times 10^4$) and Isotropic Displacement Parameters ($\text{\AA}^2 \times 10^3$) for **6**.

Atom	x	y	z	U(eq)
H4a	8340(40)	4230(70)	4860(30)	38.0(11)
H4b	8320(30)	3140(60)	5760(30)	38.0(11)
H5a	8810(30)	250(80)	6740(30)	38.1(11)
H5b	9990(30)	1140(70)	6975(19)	38.1(11)
H7a	510(50)	-1490(50)	2897(17)	45.1(12)
H7b	810(50)	-1390(50)	4010(20)	45.1(12)
H3a	9760(30)	3200(40)	3970(40)	41.9(11)
H3b	9770(30)	5260(40)	3710(40)	41.9(11)
H6a	7139(6)	7390(70)	6660(40)	38.0(10)
H6b	8350(30)	8120(60)	7200(30)	38.0(10)

H8a	820(50)	-70(40)	4510(30)	38.7(11)
H8b	570(50)	500(60)	5440(20)	38.7(11)
H8	2260(30)	2450(50)	5270(20)	1(7)

NMR, IR Spectra, HRMS & TG-DSC plots for 2-6.

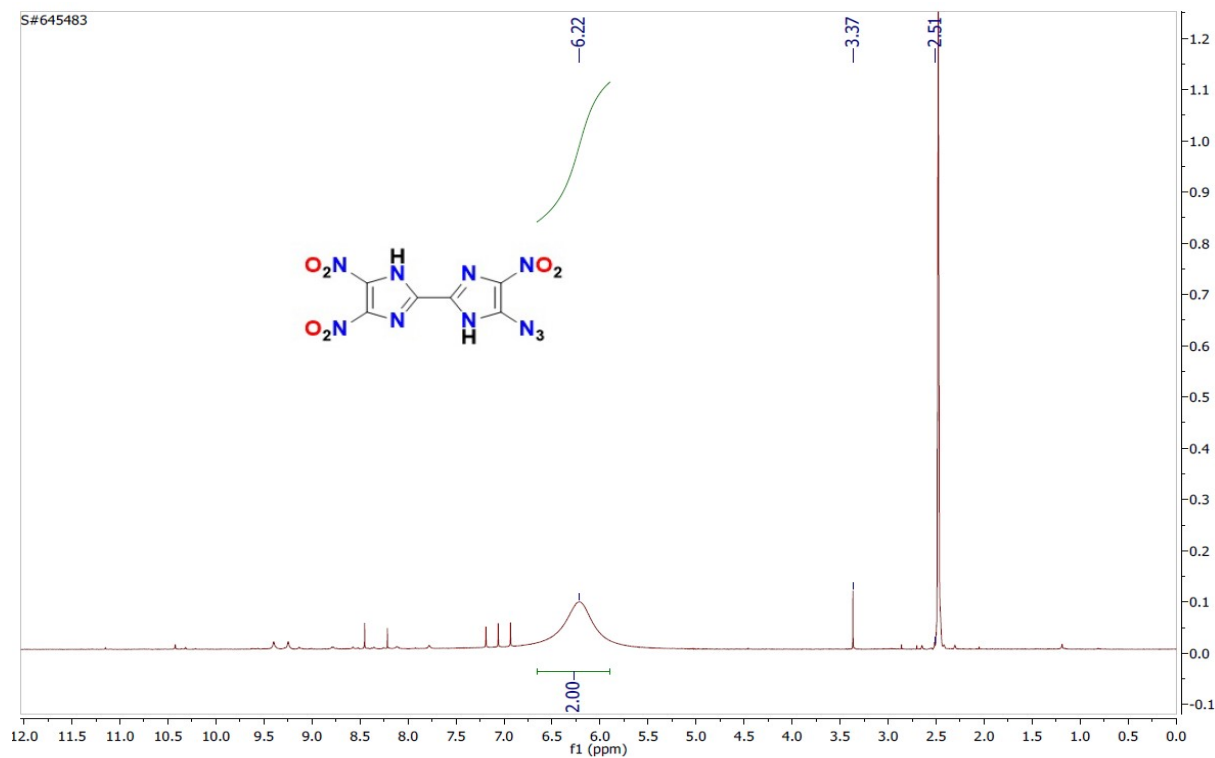


Figure S2: ^1H NMR spectrum of compound 2 in $\text{DMSO-}d_6$.

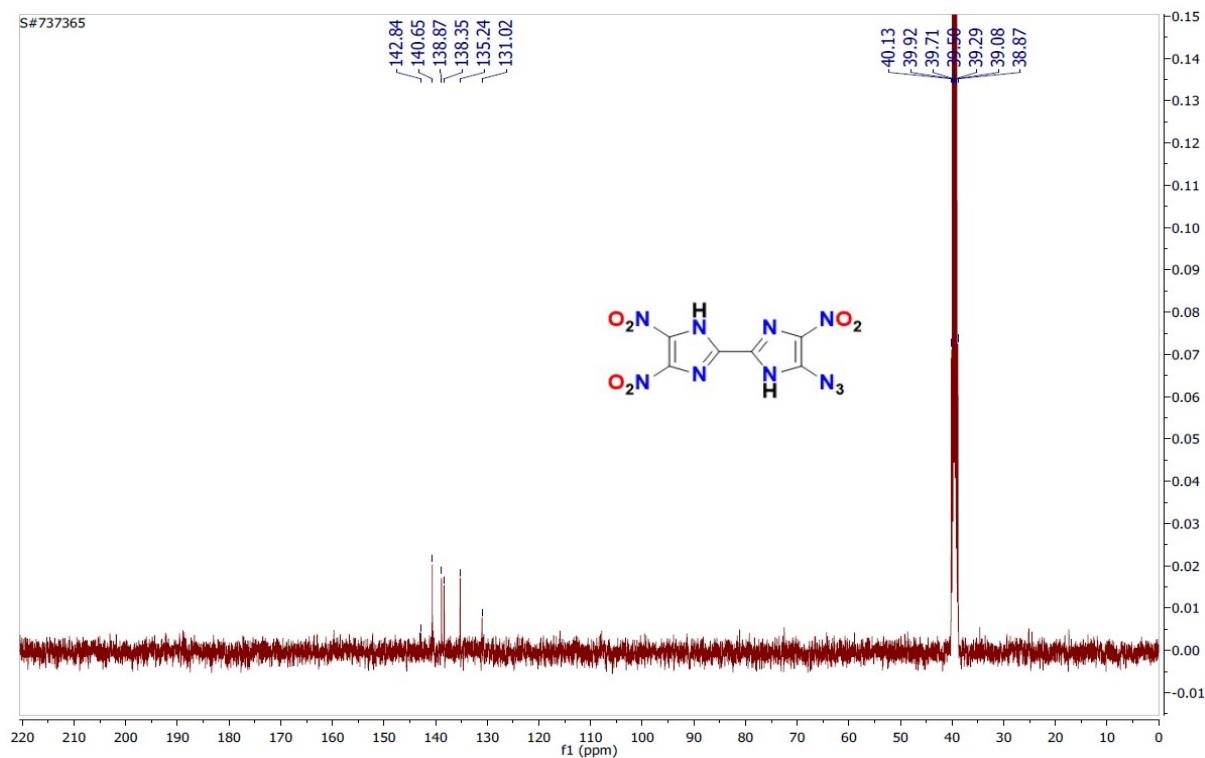


Figure S3: ^{13}C NMR spectrum of compound 2 in $\text{DMSO-}d_6$.

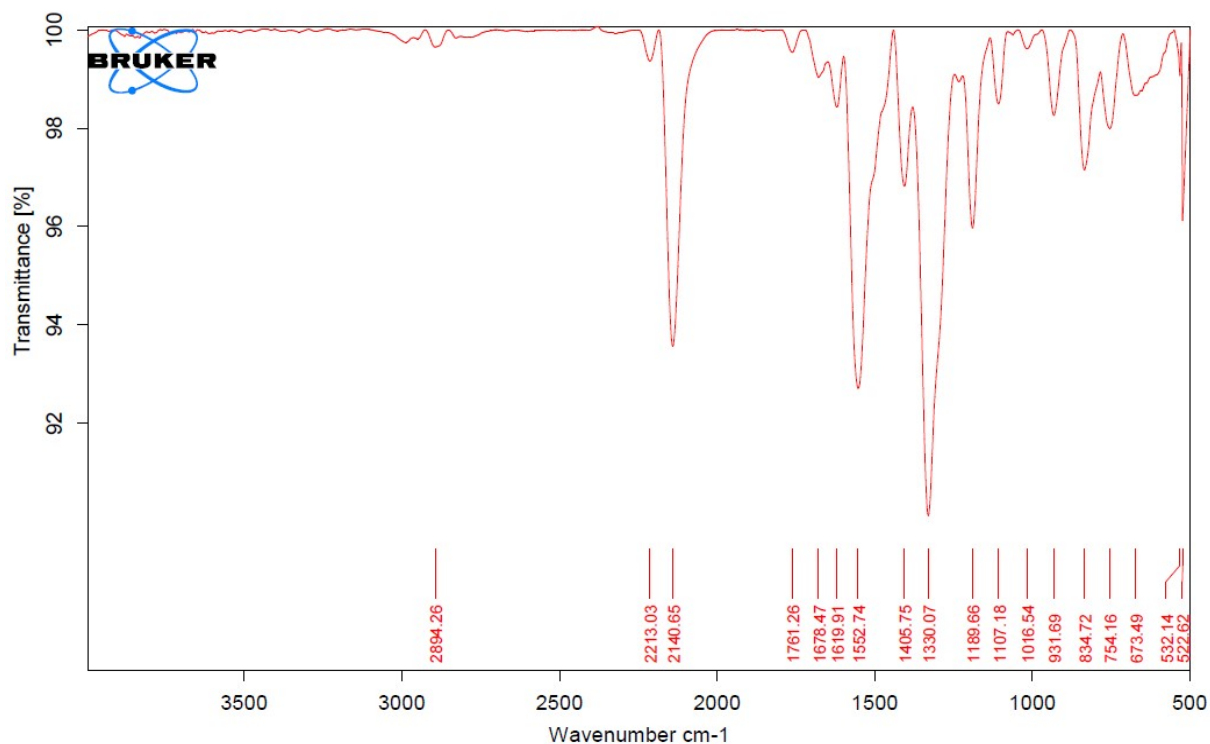


Figure S4: IR spectrum of compound 2.

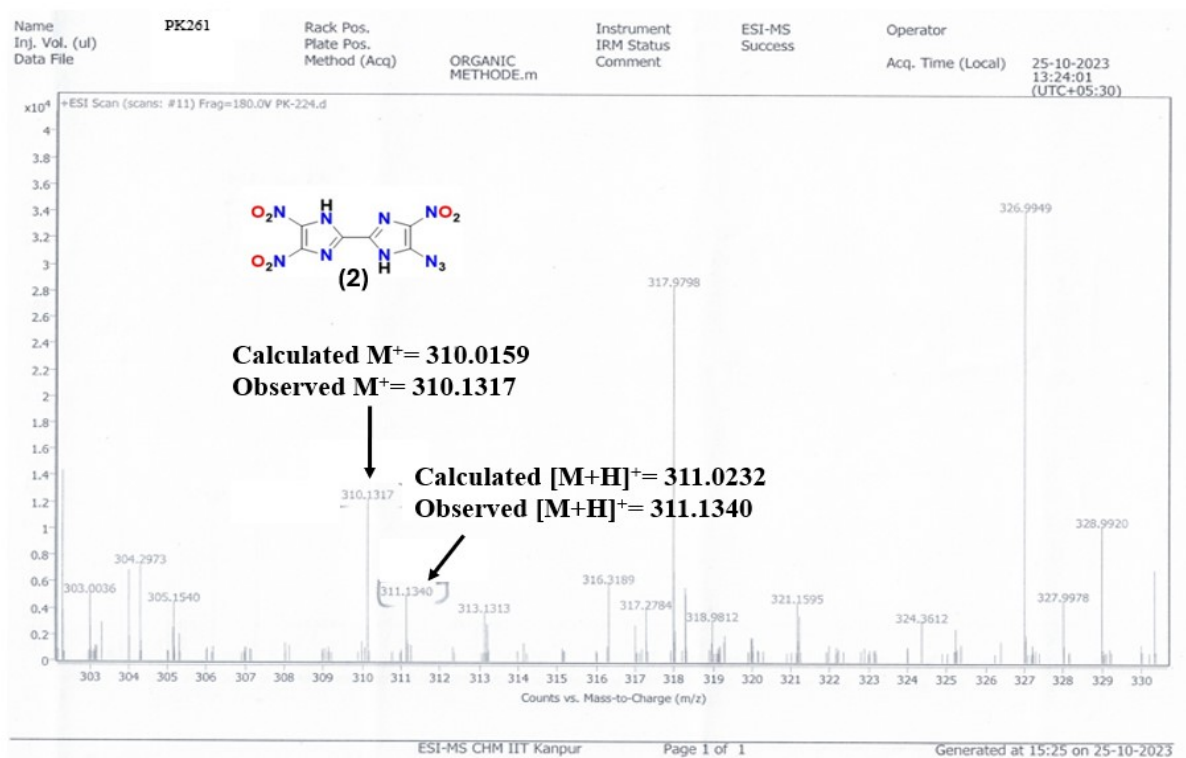
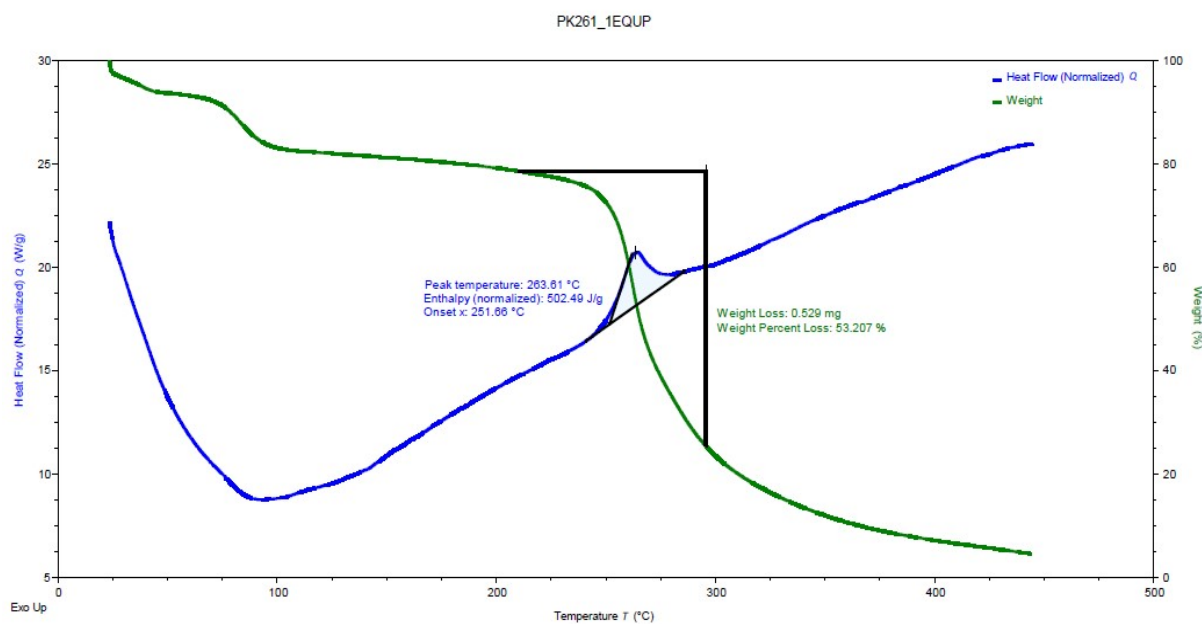


Figure S5: HRMS spectrum of compound 2.



TA Instruments Trios V5.5.0.323

Figure S6: DSC spectra of compound **2** at heating rate 5 °C min⁻¹.

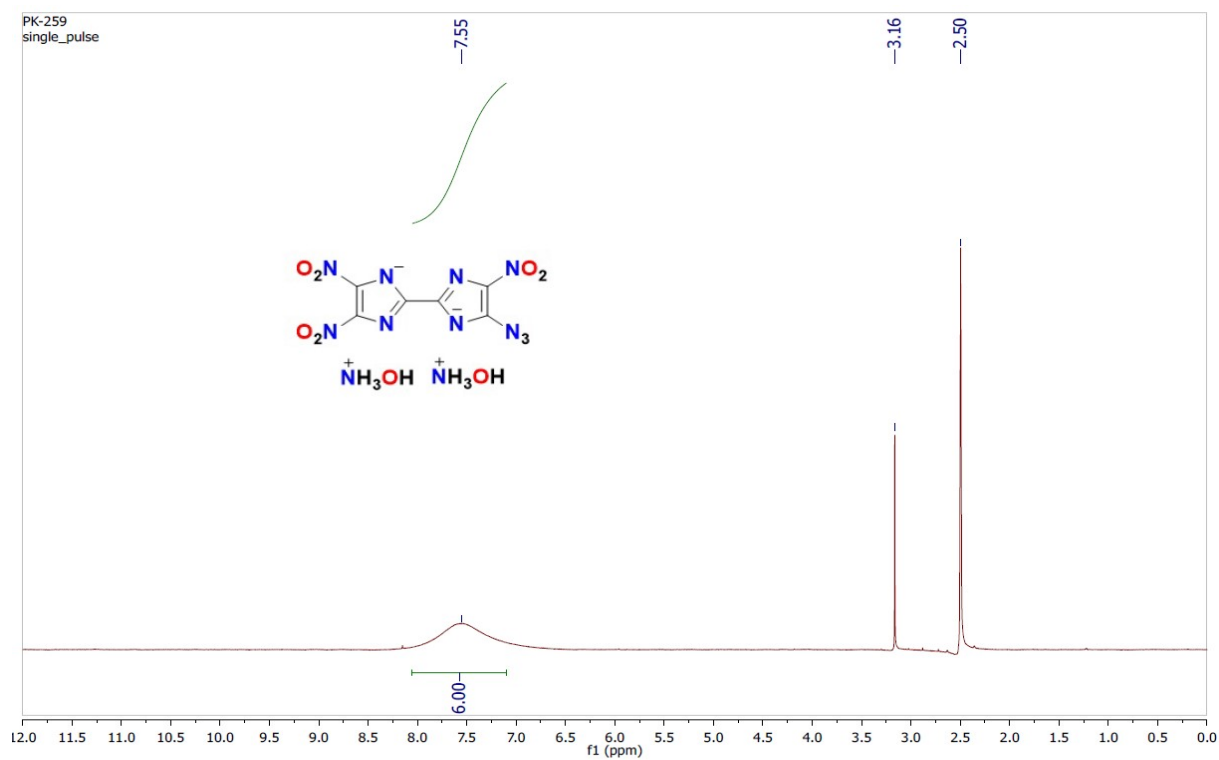


Figure S7: ¹H NMR spectrum of compound **3** in DMSO-*d*₆.

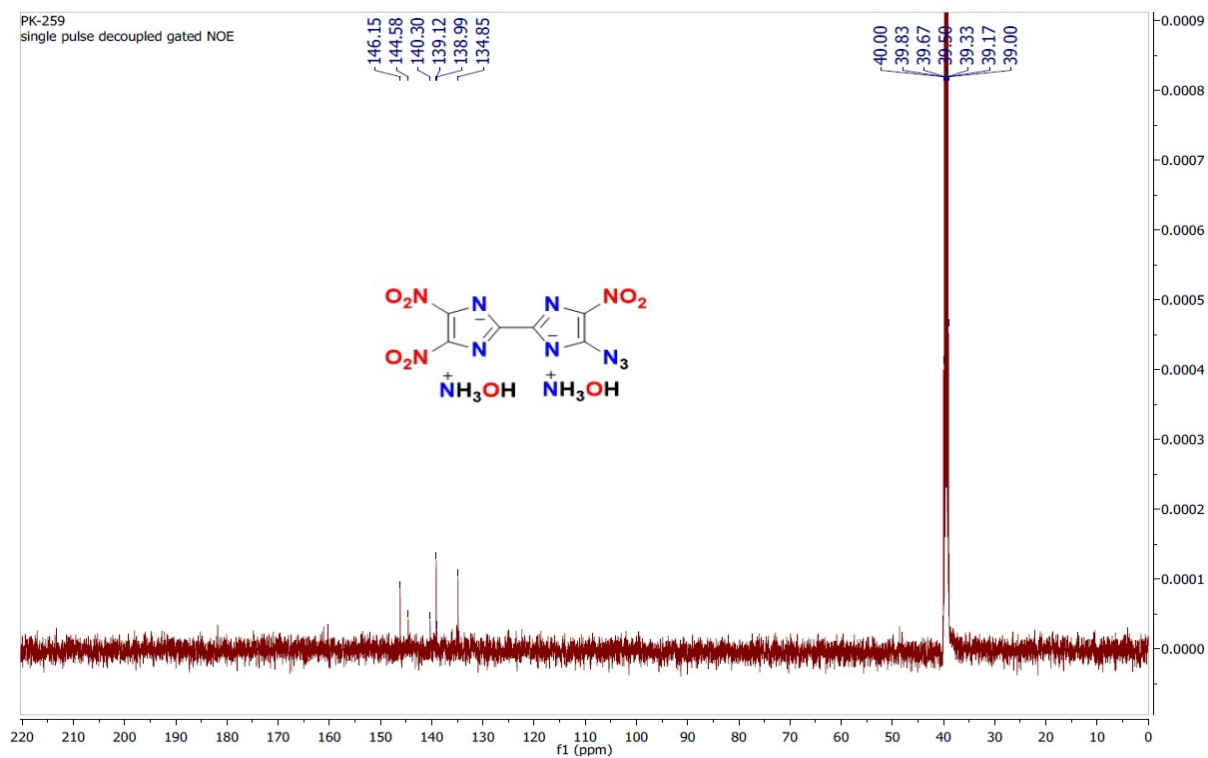


Figure S8: ^{13}C NMR spectrum of compound 3 in $\text{DMSO-}d_6$.

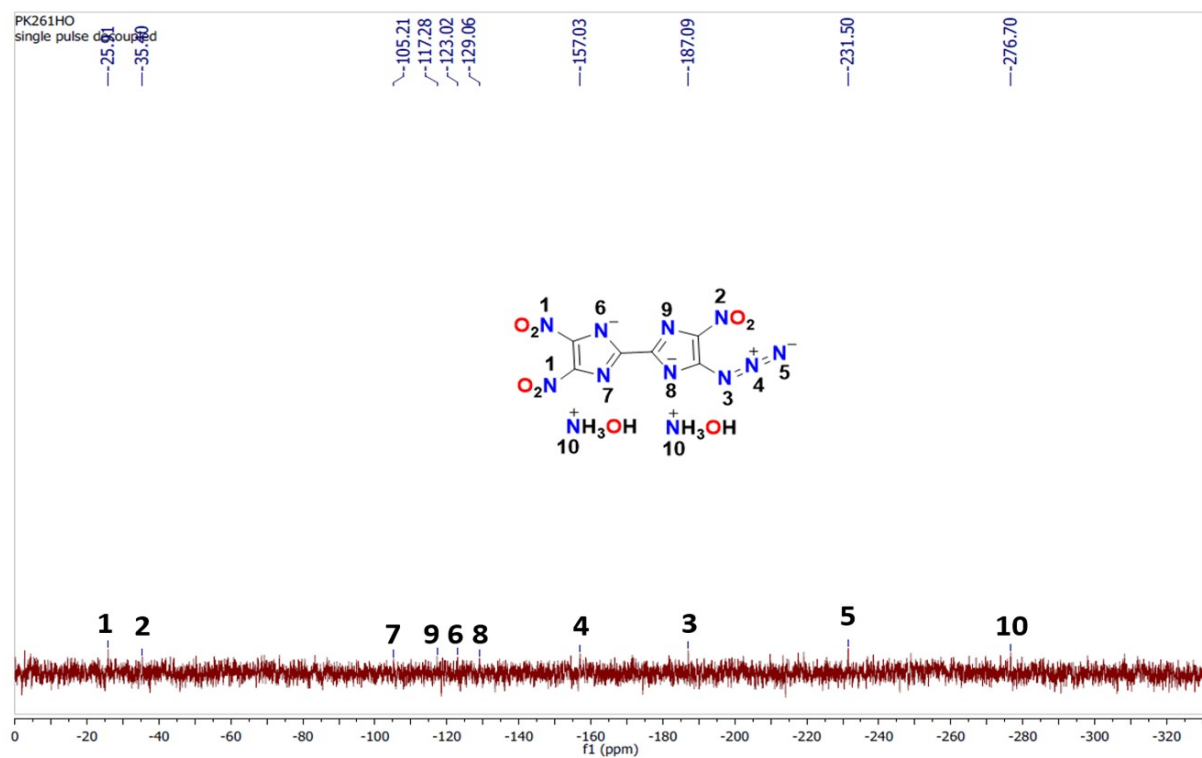


Figure S9: ^{15}N NMR spectrum of compound 3 in $\text{DMSO-}d_6$.

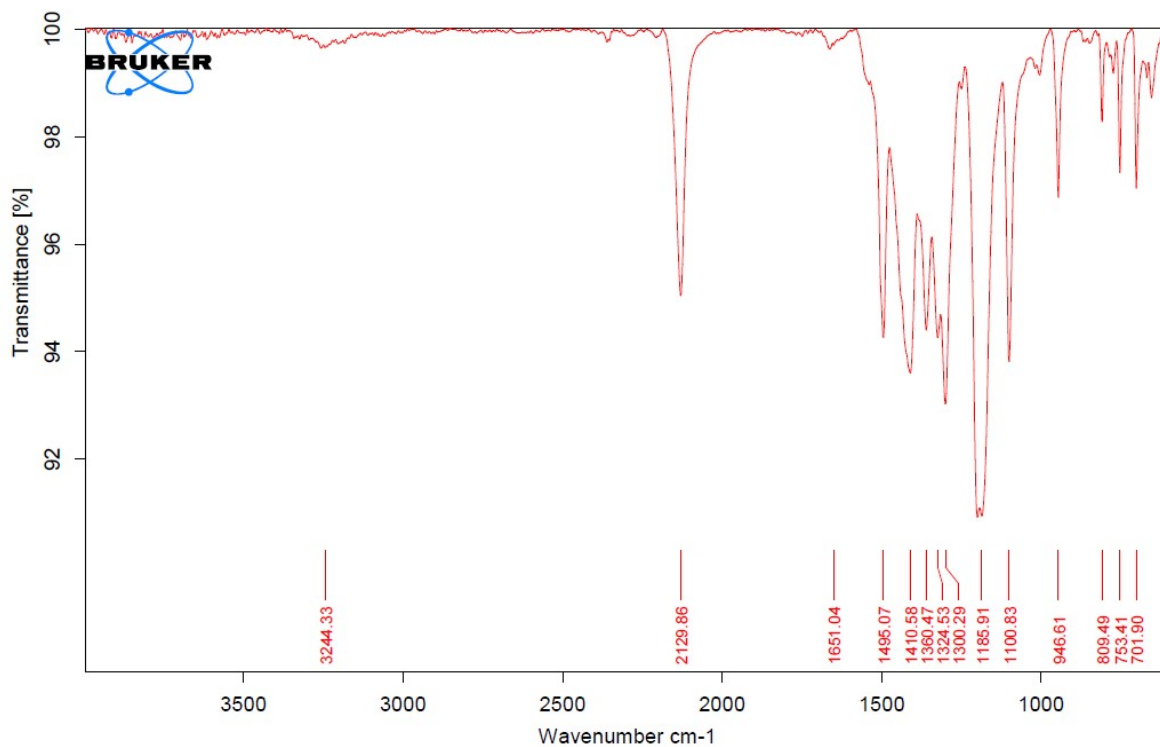
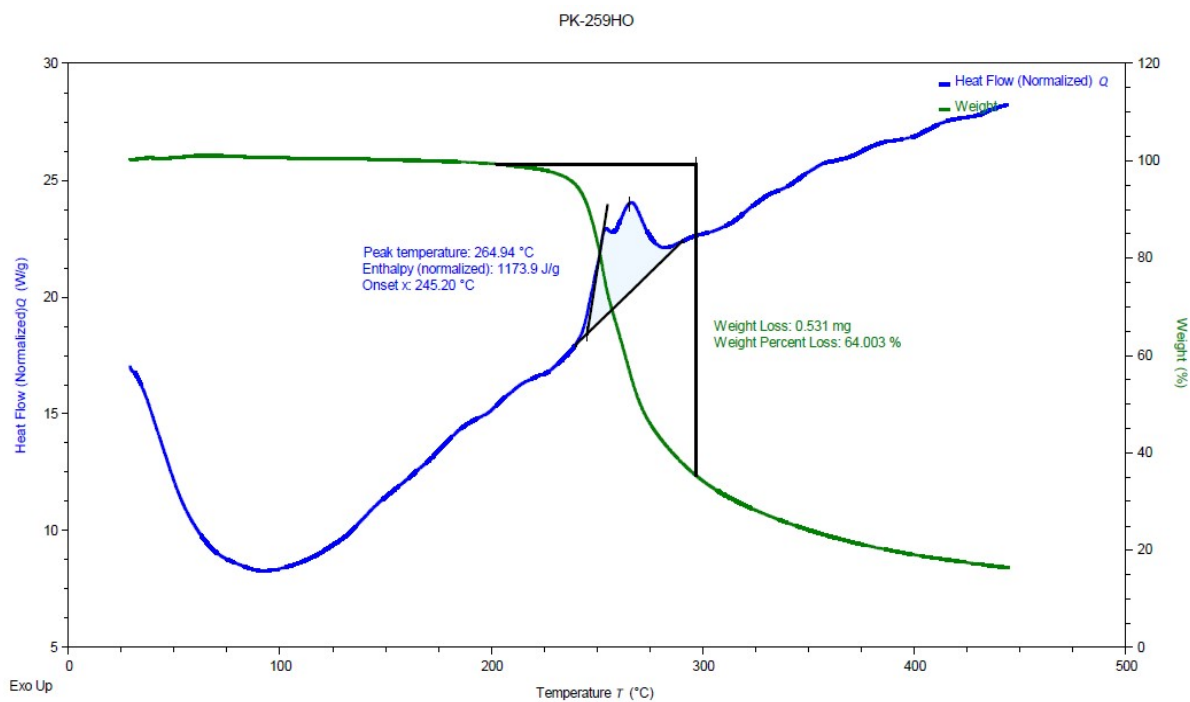


Figure S10: IR spectrum of compound **3**.



TA Instruments Trios V5.5.0.323

Figure S11: DSC spectra of compound **3** at heating rate 5 °C min^{-1} .

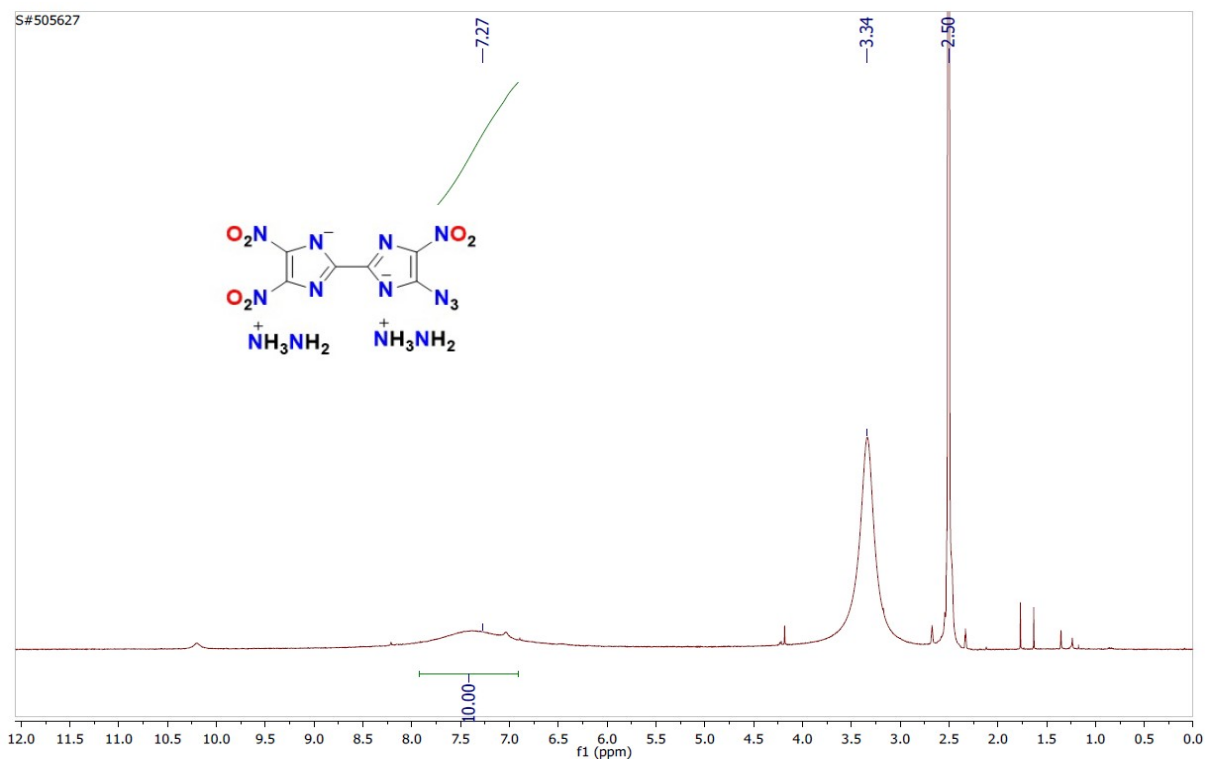


Figure S12: ^1H NMR spectrum of compound 4 in $\text{DMSO-}d_6$.

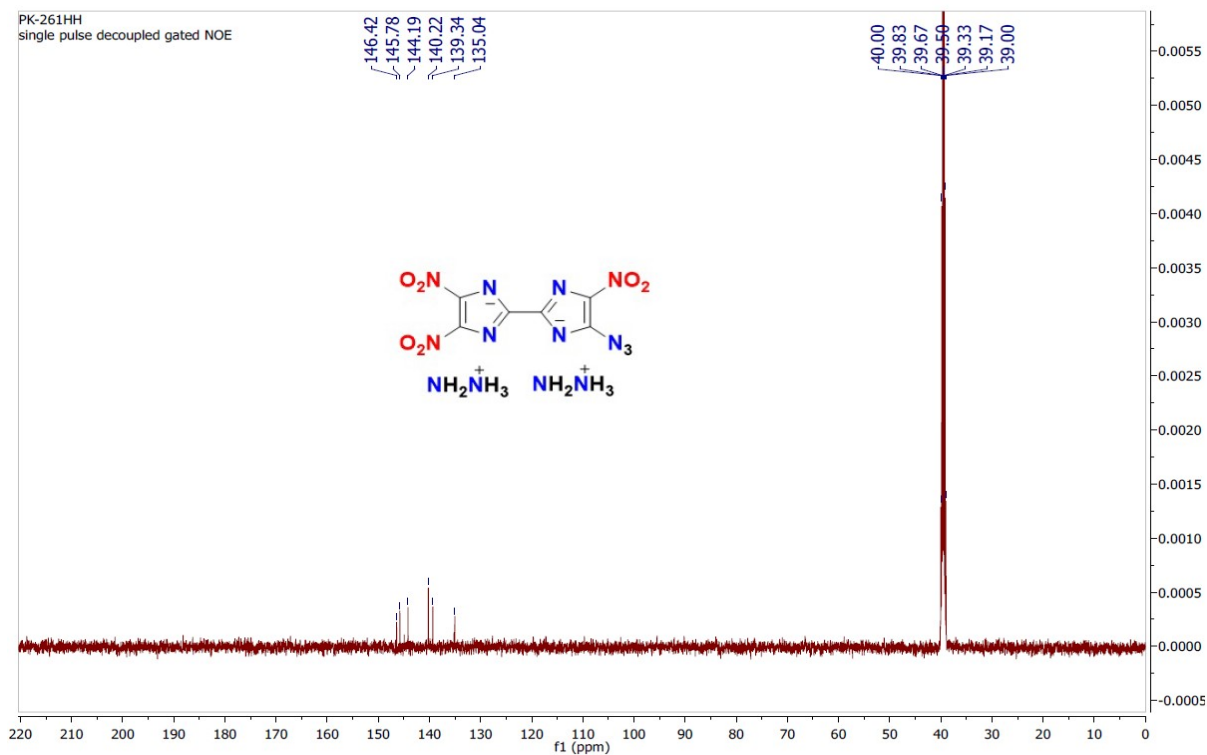


Figure S13: ^{13}C NMR spectrum of compound 4 in $\text{DMSO-}d_6$.

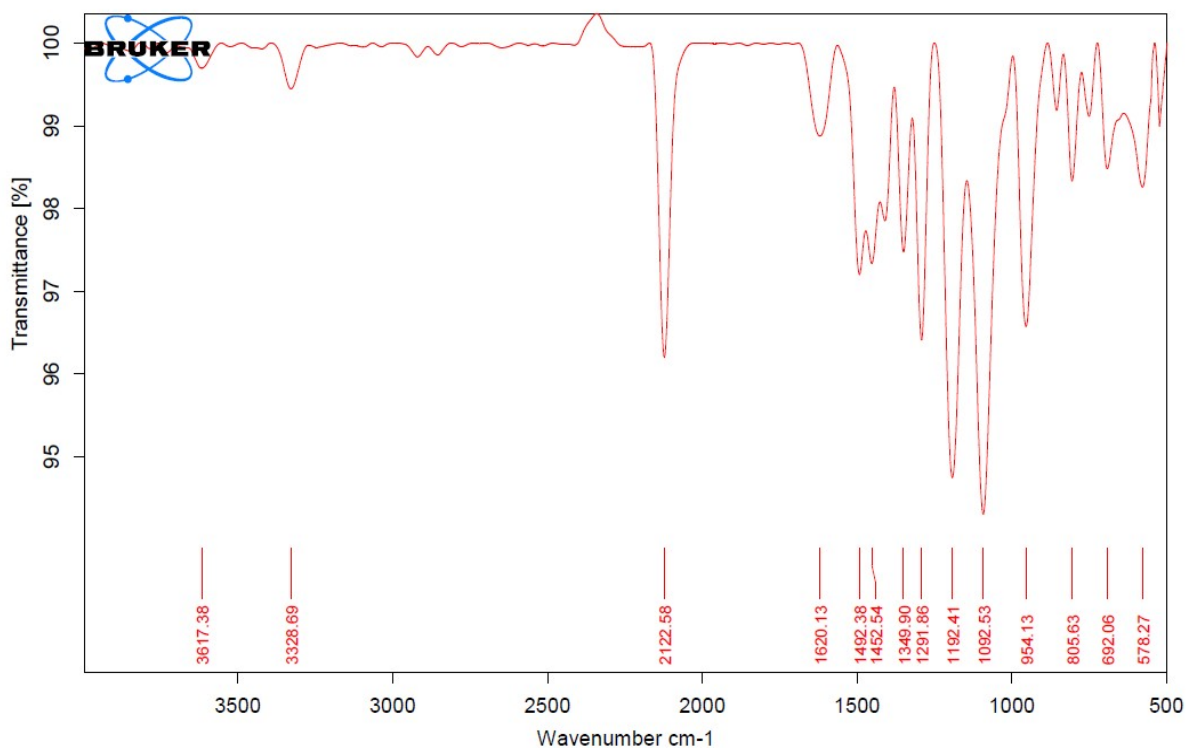
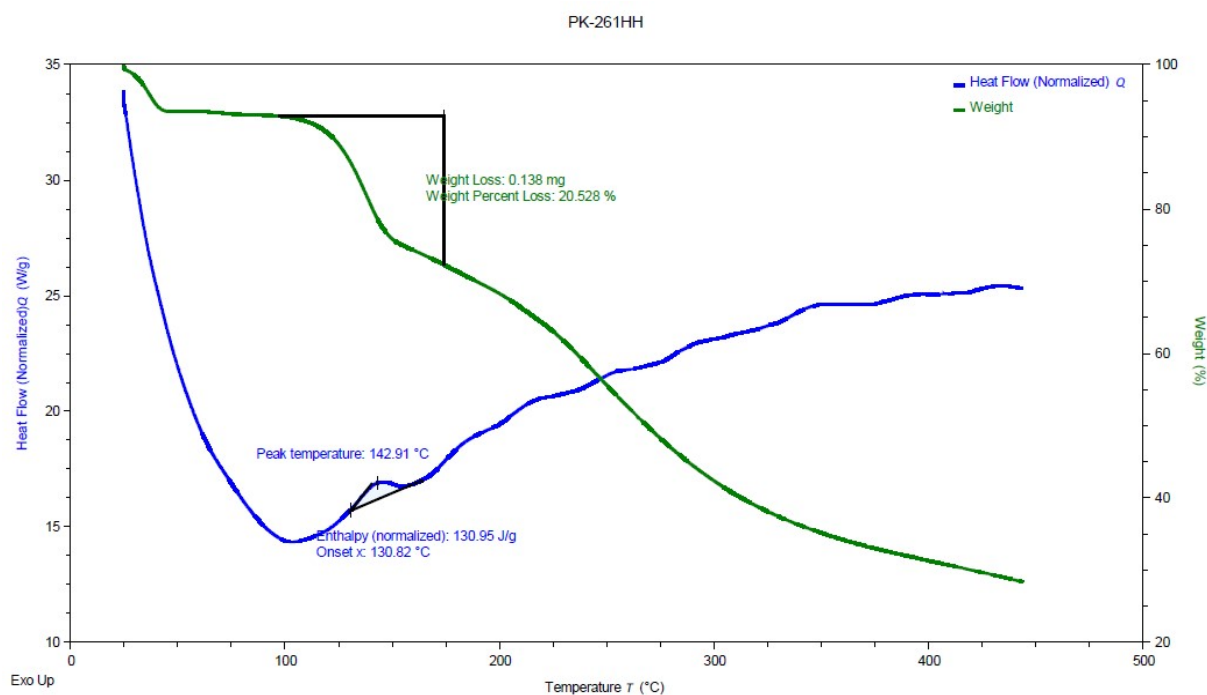


Figure S14: IR spectrum of compound 4.



TA Instruments Trios V5.5.0.323

Figure S15: DSC spectra of compound 4 at heating rate $5^{\circ}\text{C min}^{-1}$.

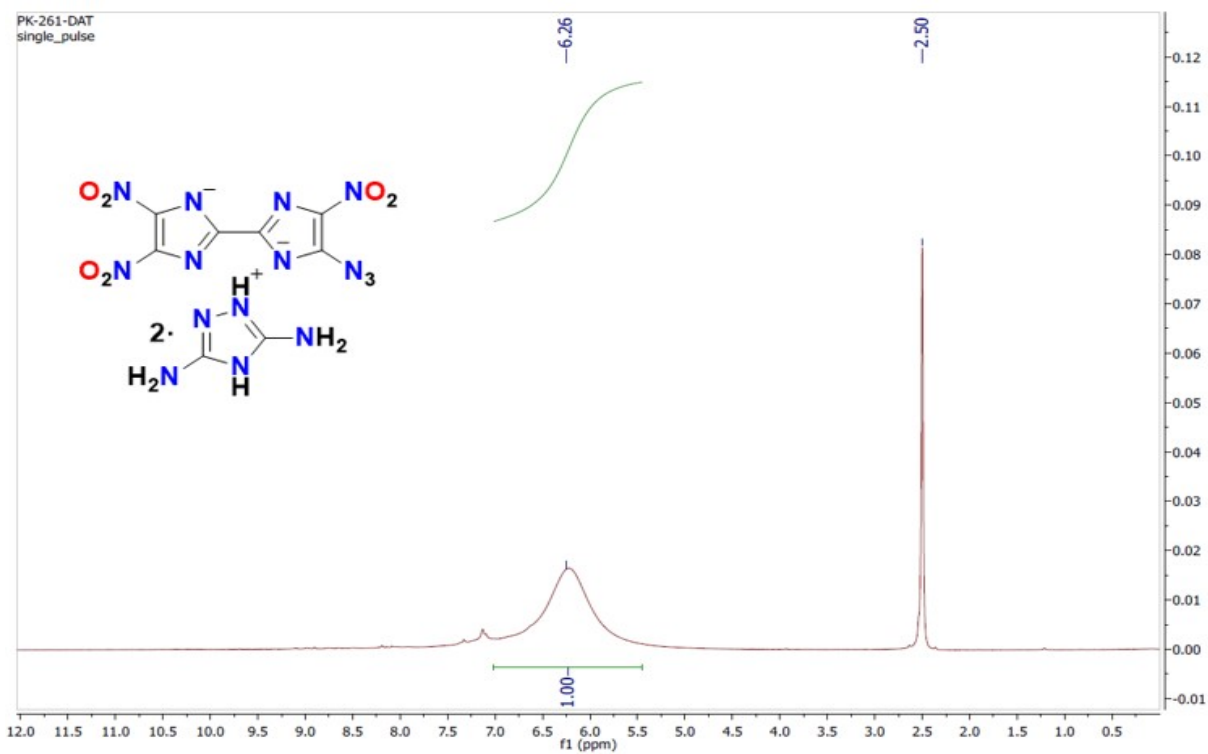


Figure S16: ^1H NMR spectrum of compound 5 in $\text{DMSO-}d_6$.

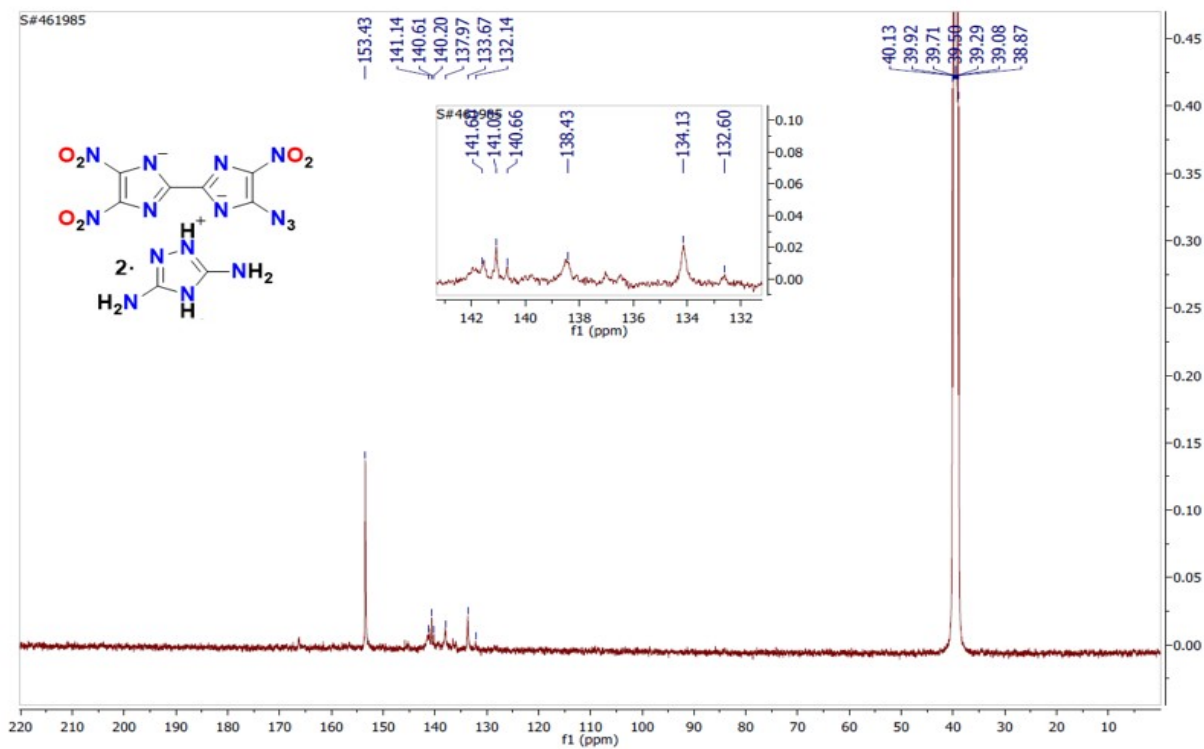


Figure S17: ^{13}C NMR spectrum of compound 5 in $\text{DMSO-}d_6$.

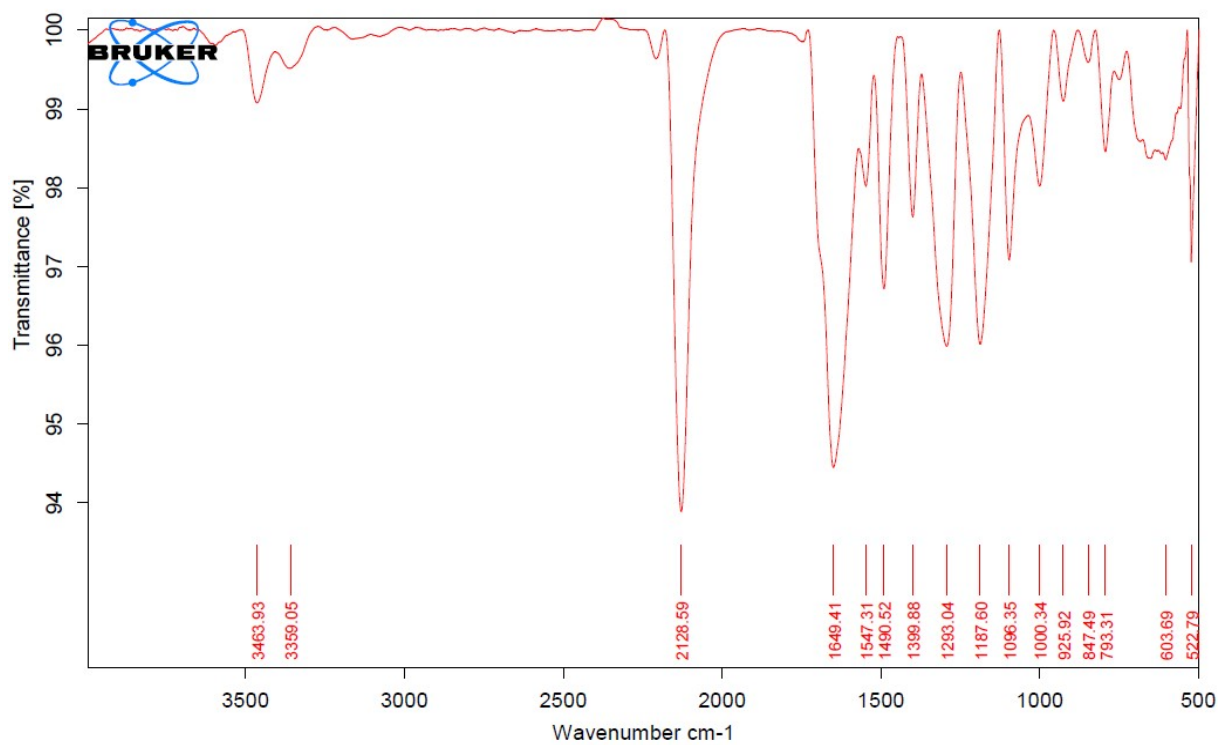
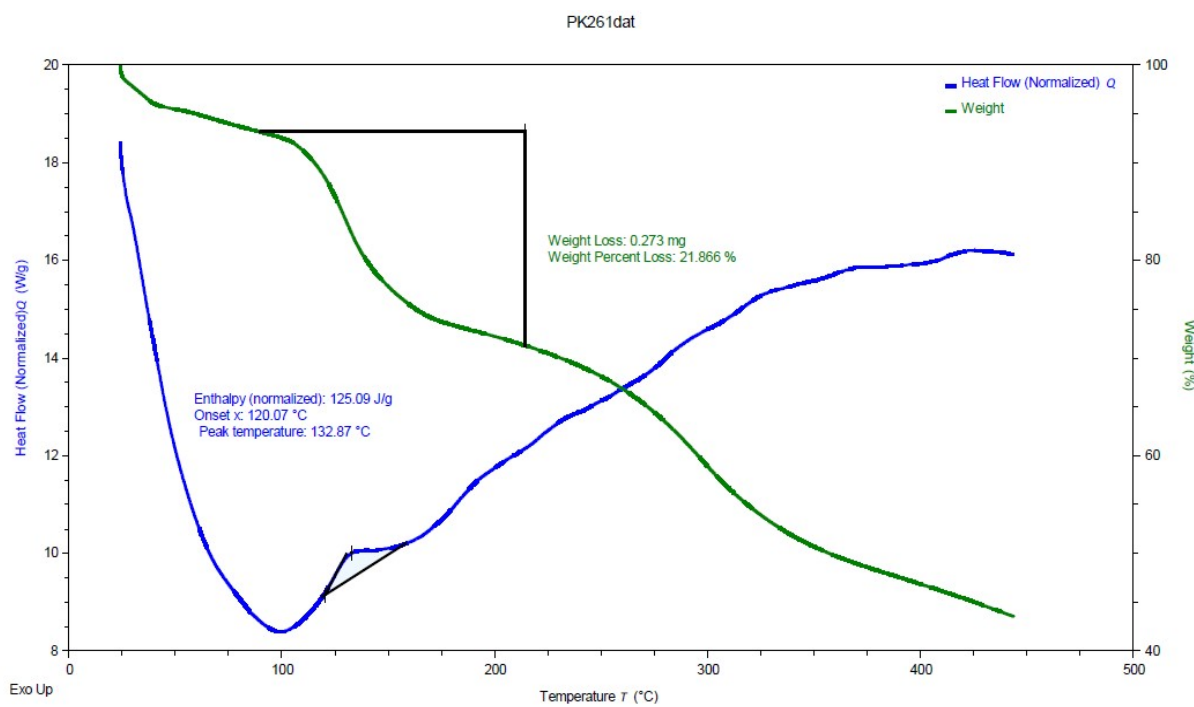


Figure S18: IR spectrum of compound **5**.



TA Instruments Trios V5.5.0.323

Figure S19: DSC spectra of compound **5** at heating rate 5 °C min^{-1} .

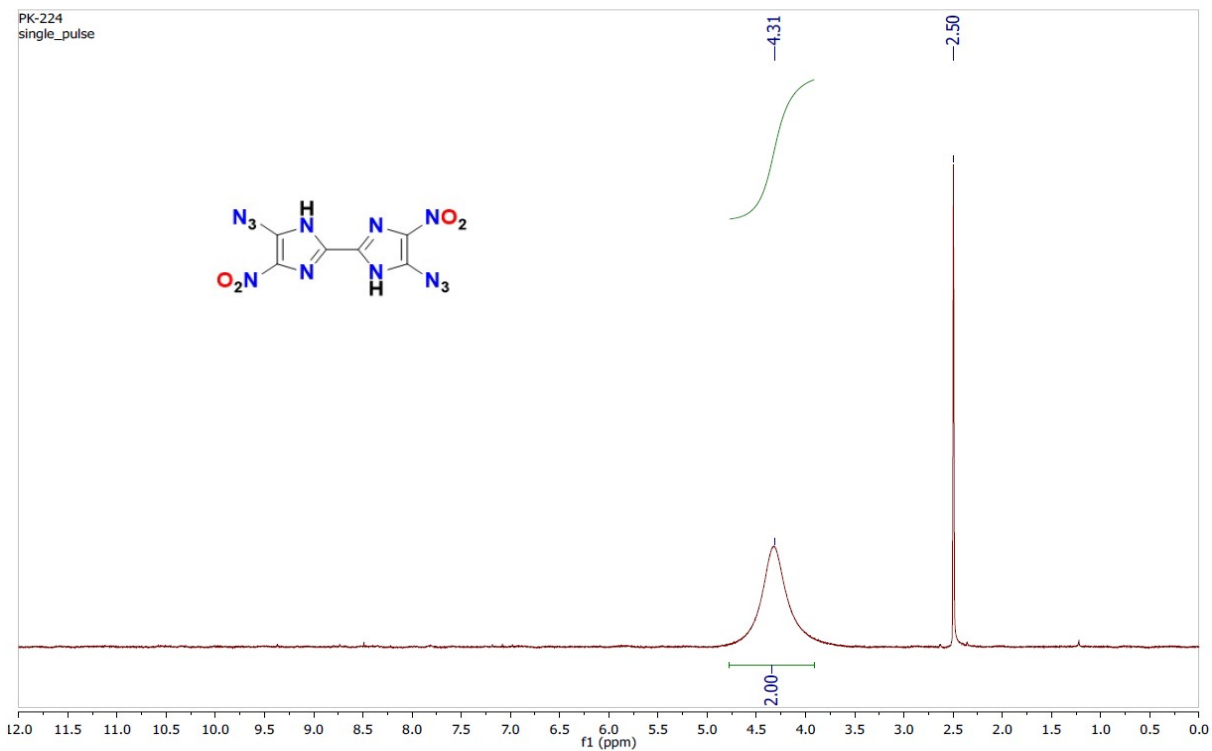


Figure S20: ^1H NMR spectrum of compound **6** in $\text{DMSO-}d_6$.

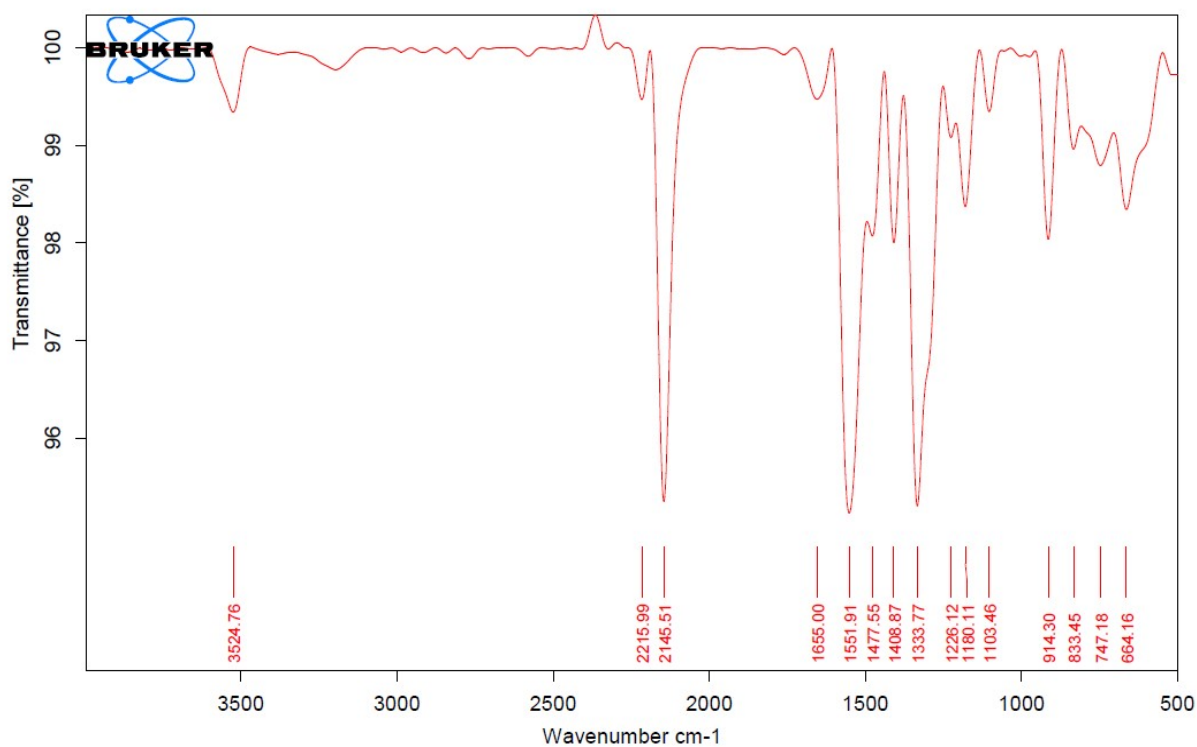


Figure S21: IR spectrum of compound **6**.

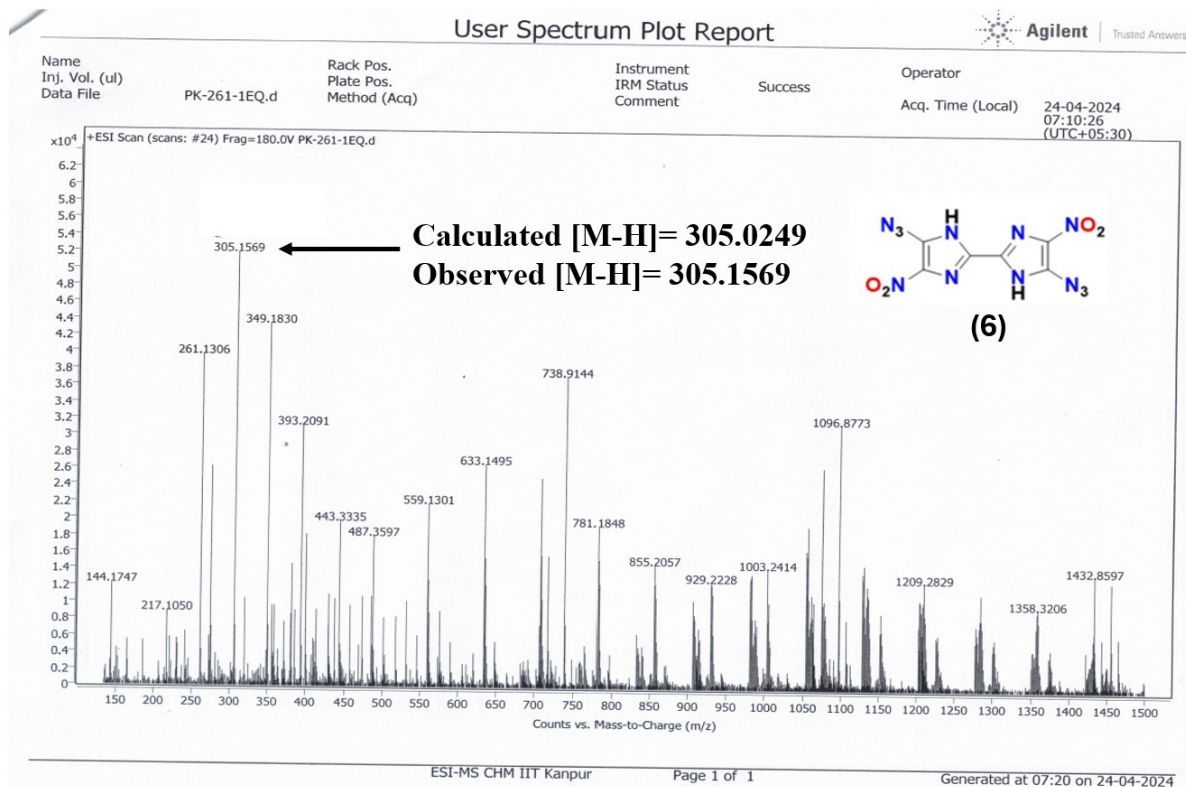


Figure S22: Mass spectrum of compound 6.

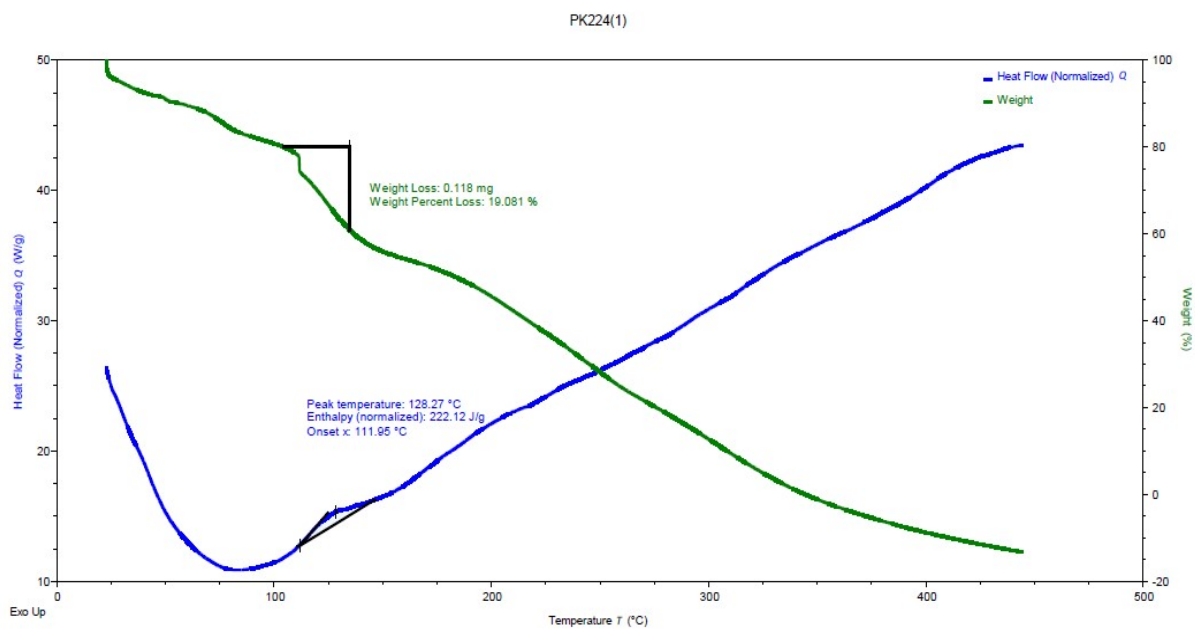
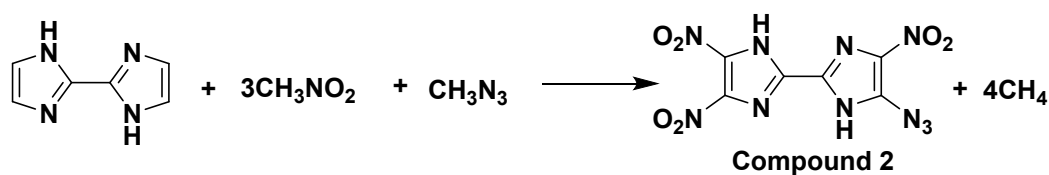


Figure S23: DSC spectra of compound 6 at heating rate 5 °C min⁻¹.

Computational Details

Computations were carried out using the Gaussian 09 program suite.³ The structure optimizations are performed with M06-2X/def2-TZVPP level of theory and characterized to be true local energy minima on the potential energy surface and no imaginary frequencies were found. Heat of formation (HOF) is a measure of energy content of an energetic material that can decompose, ignite and explode by heat or impact. It enters into the calculation of explosive and propellant properties such as detonation velocity, detonation pressure, heat of detonation and specific impulse. However, it is impractical to determine the HOF of novel energetic materials because of their unstable intermediates and unknown combustion mechanism. The calculated total energies (E_0), zero-point energies (ZPE), and thermal corrections (H_T) at the M06-2X/def2-TZVPP level for the reference compounds used in isodesmic reactions are listed in Table S9. Table S10 lists the total energies (E_0), zero-point energies (ZPE), and thermal corrections (H_T) for target compounds. HOF_{Gas} has been predicted by designing appropriate isodesmic reactions (see Figure S24). In an isodesmic reaction, the number of each kind of formal bond is conserved according to bond separation reaction (BSR) rules. The target molecule is broken down into a set of heavy atom molecules containing same component bonds. BSR rules cannot be applied to the molecules with delocalized bonds and cage skeletons because of large, calculated errors of HOFs. In view of the above, present study involves the design of isodesmic reactions in which the numbers of all kinds of bonds keep invariable to decrease the calculation errors of HOF. Aromatic rings are kept intact while constructing isodesmic reactions.



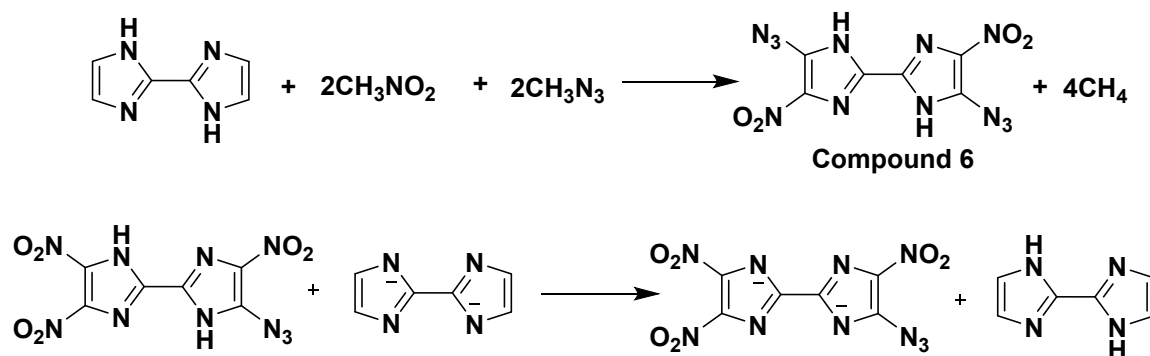


Figure S24. Designed isodesmic reactions for the prediction of gas phase heat of formation (HOF_{Gas}) of target compounds and anion.

The usage of the HOF_{Gas} in the calculation of detonation properties slightly overestimates the values of detonation velocity and detonation pressure, and hence, the solid phase HOF ($\text{HOF}_{\text{Solid}}$) has been calculated which can efficiently reduce the errors. The $\text{HOF}_{\text{Solid}}$ is calculated as the difference between HOF_{Gas} and heat of sublimation (HOF_{Sub}) as,

$$\text{HOF}_{\text{Solid}} = \text{HOF}_{\text{Gas}} - \text{HOF}_{\text{Sub}} \quad (1)$$

The heat of sublimation (HOF_{Sub}), which is required to convert the HOF_{Gas} to the $\text{HOF}_{\text{Solid}}$, was calculated from Equation (2),⁴

$$\text{HOF}_{\text{Sub}} = 0.000267 A^2 + 1.650087 (v\sigma_{\text{tot}}^2)^{0.5} - 2.966078 \quad (2)$$

Where A represents the surface area of the 0.001 electrons/bohr³ isosurface of electronic density, v denotes the degree of balance between the positive and negative surface potentials, and σ_{tot}^2 is the electrostatic potential variance. These molecular surface properties were obtained using the Multiwfn program⁵ and listed in Table S11.

Based on the Born–Haber cycle (shown in Figure S25), the heat of formation of an ionic compound can be simplified by subtracting the lattice energy of the salt (H_L) from the total heat of formation of salt (see Table S12) *i.e.* sum of the heats of formation of the cation and anion as shown in equation (3).

$$\text{HOF}(\text{salt}, 298 \text{ K}) = \text{HOF}(\text{cation}, 298 \text{ K}) + \text{HOF}(\text{anion}, 298 \text{ K}) - H_L \quad (3)$$

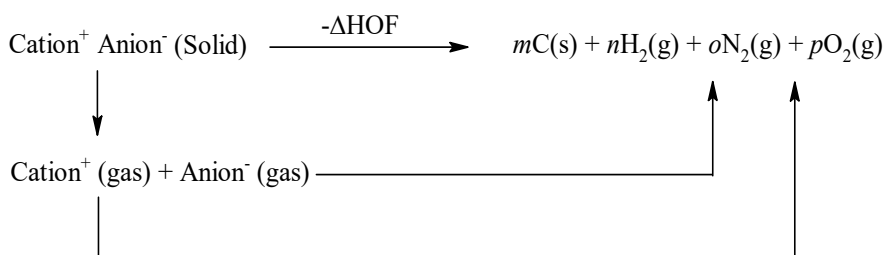


Figure S25. Born-Haber cycle for the formation of energetic salts.

Lattice potential energy is the energy associated with the process in which a crystalline solid lattice, M_pX_q is converted into its constituent gaseous ions, ${}_pM^{q+}$ (g) and ${}_qX^{p-}$ (g). The lattice energy can be predicted with reasonable accuracy by using Jenkins' equation (4).⁶

$$H_L = U_{POT} + [p(\frac{n_M}{2} - 2) + q(\frac{n_X}{2} - 2)]RT \quad (4)$$

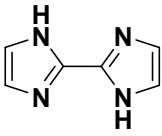
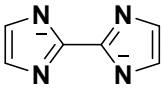
where nM and nX depend on the nature of the ions M_p^+ and X_q^- , respectively, and are equal to 3 for monoatomic ions, 5 for linear polyatomic ions, and 6 for nonlinear polyatomic ions. When lattice potential energy (U_{POT}), is incorporated and made part of a Born–Haber cycle, it needs to be converted into a lattice enthalpy term. This lattice enthalpy (H_L) involves correction of the U_{POT} term by an appropriate number of RT terms. The U_{POT} (kJ mol^{-1}) can be predicted from four different equation (5) as suggested by Jenkins et al.⁶ using following equations,

$$U_{POT} = \gamma(\frac{\rho}{M})^{1/3} + \delta \quad (5)$$

In above equation, ρ is the density (g cm^{-3}).

Table S9. Calculated total energies at 298K (E_0), zero-point energies (ZPE), and thermal corrections (H_T) and experimental HOF_{gas} of reference compounds used isodesmic reaction at the M06-2X/def2-TZVPP level.

Compd.	E_0 (a.u.)	ZPE (au)	H_T (au)	HOF_{gas} (kJ/mol)
CH ₄	-40.453065	0.0449	0.0038	-74.8
CH ₃ NO ₂	-244.955044	0.0506	0.0053	-81
CH ₃ N ₃	-204.029671	0.051	0.0054	298

	-451.127669	0.1251	0.0082	236.48
	-449.878421	0.096	0.008	439.29

^aCalculated using G4 method.

Table S10. Calculated total energies (E_0), zero-point energies (ZPE), and thermal corrections (H_T) for target compounds at the M06-2X/def2-TZVPP level.

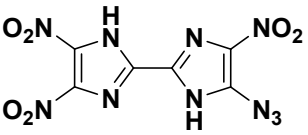
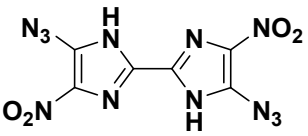
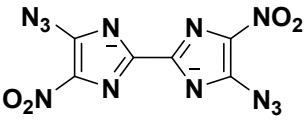
Compd.	E_0 (a.u.)	ZPE (au)	H_T (au)	HOF _{gas} /HOF _{anion} (kJ/mol)	HOF _{Sub} (kJ/mol)
	-1228.206773	0.1368	0.0185	599	141
	-1187.309704	0.1376	0.0185	904	149
	-1227.129474	0.1097	0.0181	352	-

Table S11. Calculated molecular surface properties of target compounds.

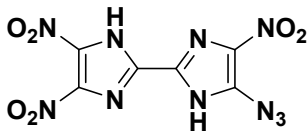
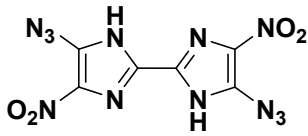
Compd.	Surface area (\AA^2)	Volume (\AA^3)	σ_{tot}^2 (kcal/mol)	ν
	277.76	281.92	221.36	0.1650
	280.11	284.65	216.40	0.2299

Table S12. Energy content of salts 3-5.

Compd.	HOF _c ^a	HOF _a ^b	U _{Pot} ^c	H _L ^d	HOF _{salt} ^e
3	675.6	352	1225	1237	466

4	769.5	352	1195	1207	684
5	775.6	352	1071	1084	819

^aHeat of formation of cation (kJ mol⁻¹). HOF_c data for cations is obtained from Ref. 5. ^bHeat of formation of anion (kJ mol⁻¹). ^cLattice potential energy (kJ mol⁻¹). ^dLattice energy (kJ mol⁻¹). ^eHeat of formation of salt (kJ mol⁻¹).

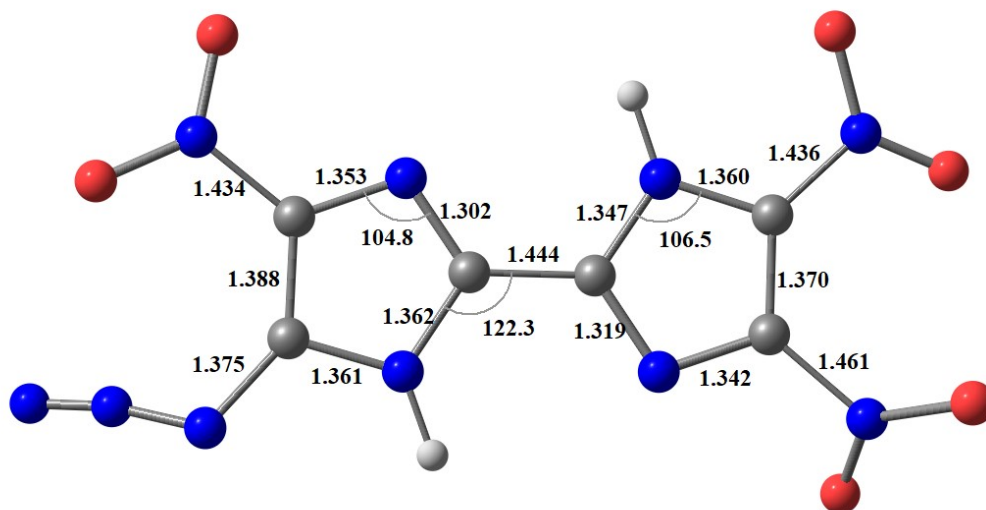


Figure S26. Selective bond lengths (Å) and angles (°) for **2**.

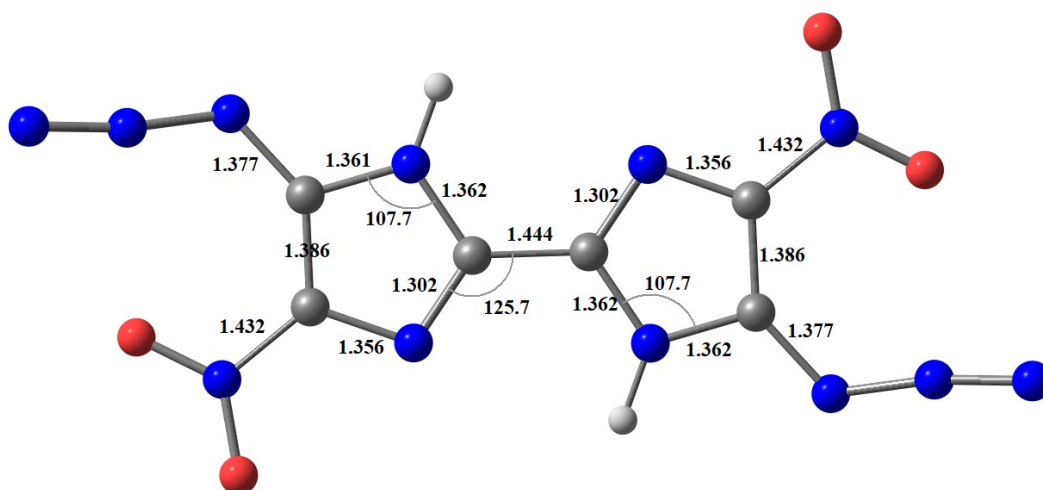


Figure S27. Selective bond lengths (Å) and angles (°) for **6**.

Table S13. Optimized coordinates of **2** at M06-2X/def2-TZVPP level of theory.

6	2.831194000	0.630609000	-0.037827000
7	1.537373000	1.048643000	-0.041351000

6	2.775130000	-0.737047000	0.028039000
6	0.776496000	-0.060896000	0.023030000
7	1.502685000	-1.161456000	0.061481000
6	-0.666518000	-0.021073000	0.043018000
7	-1.392695000	1.058808000	0.012669000
7	-1.425927000	-1.150952000	0.095176000
6	-2.670659000	0.616777000	0.052624000
6	-2.732226000	-0.769518000	0.099797000
7	3.894642000	1.587008000	-0.170975000
8	3.564987000	2.751333000	-0.069385000
8	4.999194000	1.164420000	-0.387516000
7	3.873345000	-1.697348000	0.106126000
8	4.767791000	-1.431838000	0.868519000
8	3.768845000	-2.679738000	-0.582244000
7	-3.778182000	1.525748000	0.104577000
8	-4.875496000	1.013175000	0.257756000
8	-3.559231000	2.703173000	0.008792000
7	-3.662636000	-1.778435000	0.183355000
7	-4.836626000	-1.576467000	-0.175054000
7	-5.904600000	-1.573528000	-0.468294000
1	1.226740000	2.011120000	-0.087625000
1	-1.087613000	-2.102584000	0.114194000

Table S13. Optimized coordinates of **6** at M06-2X/def2-TZVPP level of theory.

6	2.790394000	-0.722269000	-0.063517000
7	1.484013000	-1.105751000	-0.064022000
6	2.727572000	0.662554000	-0.064255000
6	0.721426000	0.023162000	-0.060010000
7	1.446139000	1.104987000	-0.055645000
6	-0.721463000	-0.023130000	-0.060067000
7	-1.446173000	-1.104961000	-0.055643000
7	-1.484052000	1.105780000	-0.064248000
6	-2.727603000	-0.662527000	-0.064402000
6	-2.790425000	0.722287000	-0.063792000
7	-3.834391000	-1.567917000	-0.135117000
8	-4.935796000	-1.053135000	-0.253416000
8	-3.615177000	-2.749456000	-0.087826000
7	3.834349000	1.567950000	-0.134917000
8	4.935768000	1.053174000	-0.253133000
8	3.615140000	2.749487000	-0.087615000
7	3.727171000	-1.730854000	-0.102459000
7	4.885816000	-1.516549000	0.292626000
7	5.943189000	-1.499088000	0.623613000
7	-3.727318000	1.730779000	-0.103060000
7	-4.885705000	1.516499000	0.292816000
7	-5.942873000	1.498976000	0.624452000
1	1.143327000	-2.056507000	-0.058151000
1	-1.143364000	2.056537000	-0.058441000

References:

1. Klapötke, T. M.; Preimesser, A.; Stierstorfer, J. Energetic Derivatives of 4, 4',5, 5'-Tetranitro-2, 2'-Bisimidazole (TNBI). *Zeitschrift für Anorg. und Allg. Chemie* **2012**, *638* (9), 1278–1286.
2. Cho, S. G.; Cho, J. R.; Goh, E. M.; Kim, J. K.; Damavarapu, R.; Surapaneni, R. Synthesis and Characterization of 4,4',5,5'-Tetranitro-2,2'-Bi-1*H*-Imidazole (TNBI). *Propellants, Explos. Pyrotech.* **2005**, *30* (6), 445–449.
3. Gaussian 09, Revision E.01, M. J.Frisch, G. W. Trucks, H. B. Schlegel, G. E. Scuseria, M A. Robb, J. R. Cheeseman, G. Scalmani, V. Barone, B. Mennucci, G. A. Petersson, H. Nakatsuji, M Caricato, X. Li, H. P. Hratchian, A. F. Izmaylov, J. Bloino, G. Zheng, J. L. Sonnenberg, M. Hada, M. Ehara, K. Toyota, R. Fukuda, J. Hasegawa, M. Ishida, T. Nakajima, Y. Honda, O. Kitao, H. Nakai, T. Vreven, Jr. J. A. Montgomery, J. E. Peralta, F. Ogliaro, M. Bearpark, J. J. Heyd, E. Brothers, K. N. Kudin, V. N. Staroverov, R. Kobayashi, J. Normand, K. Raghavachari, A. Rendell, J. C. Burant, S. S. Iyengar, J. Tomasi, M. Cossi, N. Rega, J. M. Millam, M. Klene, J. E. Knox, J. B. Cross, V. Bakken, C. Adamo, J. Jaramillo, R. Gomperts, R. E. Stratmann, O. Yazyev, A. J. Austin, R. Cammi, C. Pomelli, J. W. Ochterski, R. L. Martin, K. Morokuma, V. G. Zakrzewski, G. A. Voth, P. Salvador, J. J. Dannenberg, S. Dapprich, A. D. Daniels, O. Farkas, J. B. Foresman, J. V. Ortiz, J. Cioslowski, D. J. Fox, *Gaussian, Inc.*, Wallingford CT, **2013**.
4. Byrd, E. F. C.; Rice, B. M.; *J. Phys. Chem. A* **2006**, *110*, 1005-1013.
5. Lu, T.; Chen, F.; *J. Comput. Chem.* **2012**, *33*, 580.
6. Jenkins, H. D. B.; Tudela, D.; Glasser, L. Lattice Potential Energy Estimation for Complex Ionic Salts from Density Measurements. *Inorg. Chem.* **2002**, *41*, 2364-2367.